Greenhouse gas fluxes in mangrove forest soil in an Amazon estuary

Saúl Edgardo Martínez Castellón[1], José Henrique Cattanio[1*], José Francisco Berrêdo[1;3], Marcelo Rollnic[2], Maria de Lourdes Ruivo[1;3], Carlos Noriega[2].

[1] Graduate Program in Environmental Sciences. Federal University of Pará, Belém, Brazil

[2] Marine Environmental Monitoring Research Laboratory. Federal University of Pará, Belém, Brazil.

[3] Department of Earth Sciences and Ecology. Paraense Emílio Goeldi Museum, Belém, Brazil

[*] Corresponding author: cattanio@ufpa.br (J.H. Cattanio)

Abstract: Tropical mangrove forests are important carbon sinks, the soil being the main carbon reservoir. Understanding the variability and the key factors that control fluxes is critical to accounting for greenhouse gas (GHG) emissions, particularly in the current scenario of global climate change. This study is the first to quantify carbon dioxide (CO_2) and methane (CH_4) emissions using a dynamic chamber in a natural mangrove soil of the Amazon. The plots for the trace gases study were allocated at contrasting topographic heights. The results showed that the mangrove soil of the Amazon estuary is a source of CO_2 (6.66 g CO_2 m^{-2} d^{-1}) and CH_4 (0.13 g CH_4 m^{-2} d^{-1}) to the atmosphere. The CO_2 flux was higher in the high topography (7.86 g CO_2 m^{-2} d^{-1}) than in the low topography (4.73 g CO_2 m^{-2} d^{-1}) in the rainy season, and CH_4 was higher in the low topography (0.13 g CH_4 m^{-2} d^{-1}) than in the high topography (0.01 g CH_4 m^{-2} d^{-1}) in the dry season. However, in the dry period, the low topography soil produced more CH_4. Soil organic matter, carbon and nitrogen ratio (C/N), and redox potential influenced the annual and seasonal variation of CO_2 emissions; however, they did not affect CH_4 fluxes. The mangrove soil of the Amazon estuary produced 35.40 Mg CO_{2-eq} ha^{-1} y^{-1}. A total of 2.16 kg CO_2 m^{-2} y^{-1} needs to be sequestered by the mangrove ecosystem to counterbalance CH_4 emissions.

1   Introduction

Mangrove areas are estimated to be the main contributors to greenhouse gas emissions in marine ecosystems (Allen et al., 2011; Chen et al., 2012). However, mangrove forests are highly productive due to a high nutrient turnover rate (Robertson et al., 1992) and have mechanisms that maximize carbon gain and minimize water loss through plant transpiration (Alongi and Mukhopadhyay, 2015). A study conducted in 25 mangrove forests (between 30° latitude and 73° longitude) revealed that these forests are the

35   richest in carbon (C) storage in the tropics, containing on average 1,023 Mg C ha^{-1} of

36   which 49 to 98% is present in the soil (Donato et al., 2011).

37   The estimated soil CO_2 flux in tropical estuarine areas is 16.2 Tg C y^{-1} (Alongi, 2009).

38   However, soil efflux measurements from tropical mangroves revealed emissions

39   ranging from 2.9 to 11.0 g CO_2 m^{-2} d^{-1} (Castillo et al., 2017; Chen et al., 2014; Shiau

40   and Chiu, 2020). In situ CO_2 production is related to the water input of terrestrial,

41   riparian, and groundwater brought by rainfall (Rosentreter et al., 2018b). Due to the

42   periodic tidal movement, the mangrove ecosystem is daily flooded, leaving the soil

43   anoxic and consequently reduced, favoring methanogenesis (Dutta et al., 2013). Thus,

44   estuaries are considered hotspots for CH_4 production and emission (Bastviken et al.,

45   2011; Borges et al., 2015). Organic material decomposition by methanogenic bacteria in

46   anoxic environments, such as sediments, inner suspended particles, zooplankton gut

47   (Reeburgh, 2007; Valentine, 2011), and the impact of freshwater should change the

48   electron flow from sulfate-reducing bacteria to methanogenesis (Purvaja et al., 2004),

49   which also results in CH_4 formation. On the other hand, high salinity levels, above 18

50   ppt, may result in an absence of CH_4 emissions (Poffenbarger et al., 2011), since CH_4

51   dissolved in pores is typically oxidized anaerobically by sulfate (Chuang et al., 2016).

52   Currently the uncertainty in emitted CH_4 values in vegetated coastal wetlands is

53   approximately 30% (EPA, 2017). Soil flux measurements from tropical mangroves

54   revealed emissions range from 0.3 to 4.4 mg CH_4 m^{-2} d^{-1} (Castillo et al., 2017; Chen et

55   al., 2014; Kreuzwieser et al., 2003).

56   The production of greenhouse gases from soils is mainly driven by biogeochemical

57   processes. Microbial activities and gas production are related to soil properties,

58   including total carbon and nitrogen concentrations, moisture, porosity, salinity, and

59   redox potential (Bouillon et al., 2008; Chen et al., 2012). Due to the dynamics of tidal

60   movements, mangrove soils may become saturated and present reduced oxygen

61   availability, or suffer total aeration caused by the ebb tide. Studies attribute soil carbon

62   flux responses to moisture perturbations because of seasonality and flooding events

63   (Banerjee et al., 2016), with fluxes being dependent on tidal extremes (high tide and low

64   tide), and flood duration (Chowdhury et al., 2018). In addition, phenolic compounds

65   inhibit microbial activity and help keep organic carbon intact, thus leading to the

66   accumulation of organic matter in mangrove forest soils (Friesen et al., 2018).

The Amazonian coastal areas in the State of Pará (Brazil) cover 2,176.8 km^2 where mangroves develop under the macro-tide regime (Souza Filho, 2005), representing approximately 85% of the entire area of Brazilian mangroves (Herz, 1991). The objective of this study is to investigate the monthly flux of CO_2 and CH_4 from the soil, at two topographic heights, in a pristine mangrove area in the Mojuim River Estuary, belonging to the Amazon biome. The gas fluxes were studied together with the analysis of the vegetation structure and soil physical-chemical parameters.

2   Material and Methods

2.1   Study site

This study was conducted in the Amazonian coastal zone, Macaca Island (-0.746491 latitude and -47.997219 longitude), located in the Mojuim River estuary, at the Mocapajuba Marine Extractive Reserve, municipality of São Caetano de Odivelas (Figure 1), state of Pará (Brazil). The Macaca island has an area of 1,322 ha of pristine mangroves, and belongs to a mangrove area of 2,177 km^2 in the state of Pará (Souza Filho, 2005). The climate is type Am (tropical monsoon) according to the Köppen classification (Peel et al., 2007). The climatological data were obtained from the Meteorological Database for Teaching and Research of the National Institute of Meteorology (INMET). The area has a rainy season from January to June (2,296 mm of precipitation) and a dry season from July to December (687 mm). March and April were the rainiest months with 505 and 453 mm of precipitation, while October and November were the driest (53 and 61 mm, respectively). The minimum temperatures occur in the rainy period (26 °C) and the maximum in the dry period (29 °C). The Mojuim estuary has a macrotidal regime, with an average amplitude of 4.9 m during spring tide and 3.2 m during low tide (Rollnic et al., 2018). During the wet season the Mojuim River has a flow velocity of 1.8 m s^{-1} at the ebb tide and 1.3 m s^{-1} at the flood tide, whereas in the dry season, the maximum currents reach 1.9 m s^{-1} at the flood and 1.67 m s^{-1} at the ebb tide (Rocha, 2015). The annual mean salinity of the river water is 26.95 PSU (Valentim et al., 2018).
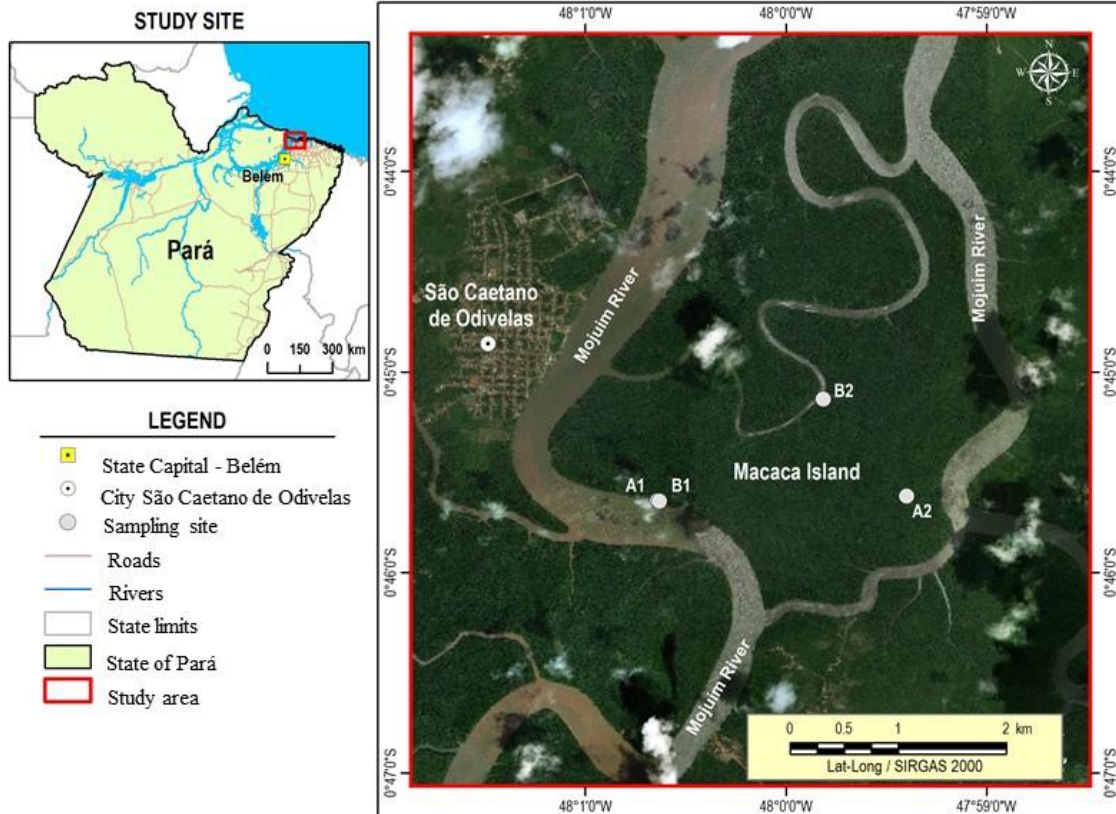
Figure 1. The Macaca Island located in the mangrove coast of Northern Brazil, Municipality of São Caetano de Odivelas (state of Pará), with sampling points at low (plot B1 and plot B2) and high (plot A1 and plot A2) topographies. Image Source: © Google Earth

The Mojuim River region is geomorphologically formed by partially submerged river basins consequent of the increase in the relative sea level during the Holocene (Prost et al., 2001) associated with the formation of mangroves, dunes, and beaches (El-Robrini et al., 2006). Before reaching the estuary, the Mojuim River crosses an area of a dryland forest highly fragmented by family farming, forming remnants of secondary forest (< 5.0 ha) of various ages (Fernandes and Pimentel, 2019). The population economically exploited the estuary, primarily by artisanal fishing, crab (*Ucides cordatus* L.) extraction, and oyster farms.

The flora of the mangrove area of Macaca Island is little anthropized and comprises the plant genera *Rhizophora*, *Avicenia*, *Laguncularia*, and *Acrostichum* (Ferreira, 2017; França et al., 2016). The estuarine plains are influenced by macrotide dynamics and can be physiographically divided into four sectors according to the different vegetation covers, associated with the landforms distribution, topographic gradient, tidal

inundation, and levels of anthropic transformation(França et al., 2016). The Macaca Island is ranked as being from the fourth sector, which implies having woods of adult trees of the genus *Ryzophora* with an average height of 10 to 25 m, is located at an elevation of 0 to 5 m, and having silt-clay soil (França et al., 2016).

Four sampling plots were selected in the Macaca Island (Figure 1) on 19/05/2017, when the moon was in the waning quarter phase: two plots where flooding occurs every day (plots B1 and B2; Figure 1), called low topography (Top_Low), and two plots where flooding occurs only at high tides during the solstice and on the high tides of the rainy season of the new and full moons (plots A1 and A2; Figure 1), called high topography (Top_High).

2.2 Greenhouse gas flux measurements

In each plot, eight Polyvinyl Chloride rings with 0.20 m diameter and 0.12 m height were randomly installed within a circumference with a diameter of 20 m. The rings had an area of 0.028 m^{-2} (volume of 3.47 L), were fixed 0.05 m into the ground, and remained in place until the study was completed. Once a month, gas fluxes were measured during periods of waning or crescent moon, as these are the times when the soil in the low topography is more exposed. To avoid the influence of mangrove roots on the gas fluxes, the rings were placed in locations without any seedlings or aboveground mangrove roots. The CO_2 and CH_4 concentrations (ppm) were measured using the dynamic chamber methodology (Norman et al., 1997; Verchot et al., 2000), sequentially connected to a Los Gatos Research portable gas analyzer (Mahesh et al., 2015). The device was calibrated monthly with a high quality standard gas (500 ppm CO_2; 5 ppm CH_4). The rings were sequentially closed for three minutes with a PVC cap, being connected to the analyzer through two 12.0 m polyethylene hoses. The gas concentration was measured every two seconds and automatically stored by the analyzer. CO_2 and CH_4 fluxes were calculated from the linear regression of increasing/decreasing CO_2 and CH_4 concentrations within the chamber, usually between one and three minutes after the ring cover was placed (Frankignoulle, 1988; McEwing et al., 2015). The flux is considered zero when the linear regression reaches an $R^2 <$ 0.30 (Sundqvist et al., 2014). However, in our analyses, most regressions reached $R^2 >$ 0.70, and the regressions were weak and considered zero in only 6% of the samples. At the end of each flux measurement, the height of the ring above ground was measured at

145   four equidistant points with a ruler. The seasonal data were analyzed by comparing the
146   average monthly fluxes in the wet season and dry season separately.

2.3   Vegetation structure and biomass

148   The floristic survey was conducted in October 2017 using circular 1,256.6 m^2 plots
149   (Kauffman et al., 2013) divided into four 314.15 m^2 subplots, which is the equivalent to
150   0.38 ha, at the same topographies as the gas flux analysis (Figure 1). We recorded the
151   diameter above the aerial roots, the diameter of the stem, and total height of all trees
152   with DBH (diameter at breast height; m) greater than 0.05m. The allometric equations
153   (Howard et al., 2014) to calculate tree biomass (aboveground biomass; AGB) were:
154     $AGB = 0.1282 * DBH^{2.6}$ ($R^2 = 0.92$) for *R. mangle*; $AGB = 0.140 * DBH^{2.4}$ ($R^2 = 0.97$)
155   for *A. germinans*; and Total $AGB = 0.168 * \rho * DBH^{2.47}$ ($R^2 = 0.99$), where $\rho_{R.\ mangle} =$
156   0.87; $\rho_{A.\ germinans} = 0.72$ (ρ = wood density).

2.4   Soil sampling and environmental characterization

158   Four soil samples were collected with an auger at a depth of 0.10 m in all the studied
159   plots for gas flux measurements (Figure 1) in July 2017 (beginning of the dry season)
160   and January 2018 (beginning of the rainy season). Before the soil samples were
161   removed, pH and redox potential (Eh; mV) were measured with a Metrohm 744
162   equipment by inserting the platinum probe directly into the intact soil at a depth of 0.10
163   m (Bauza et al., 2002). The soil samples collected in the field were transported to the
164   laboratory (Chemical Analysis Laboratory of the *Museu Paraense Emílio Goeldi*) in
165   thermal boxes containing ice. The soil samples were analyzed on the day after collection
166   at the laboratory, and the samples were kept in a freezer. Salinity (Sal; ppt) was
167   measured with PCE-0100, and soil moisture (Sm; %) by the residual gravimetric
168   method (EMBRAPA, 1997).

169   Organic Matter (OM; g kg^{-1}), Total Carbon (T_C; g kg^{-1}) and Total Nitrogen (T_N; g kg^{-1})
170   were calculated by volumetry (oxidoreduction) using the Walkley-Black method
171   (Kalembasa and Jenkinson, 1973). Microbial carbon (C_{mic}; mg kg^{-1}) and microbial
172   nitrogen (N_{mic}; mg kg^{-1}) were determined through the 2.0 min of Irradiation-extraction
173   method of soil by microwave technique (Islam and Weil, 1998). Microwave heated soil
174   extraction proved to be a simple, fast, accurate, reliable, and safe method to measure
175   soil microbial biomass (Araujo, 2010; Ferreira et al., 1999; Monz et al., 1991). The C_{mic}
176   was determined by dichromate oxidation (Kalembasa and Jenkinson, 1973; Vance et al.,

177 1987). The N_{mic} was analyzed following the method described by Brookes et al. (1985),
178 changing fumigation to irradiation, which uses the difference between the amount of T_N
179 in irradiated and non-irradiated soil. We used the flux conversion factor of 0.33
180 (Sparling and West, 1988) and 0.54 (Almeida et al., 2019; Brookes et al., 1985), for
181 carbon and nitrogen, respectively. Particle size analysis was performed separately on
182 four soil samples collected at each flux plot, in the two seasons (October 2017 and
183 March 2018), according to EMBRAPA (1997).

184 At each gas flux measurement, environmental variables such as air temperature (T_{air},
185 °C), relative humidity (RH, %), and wind speed (W_s, m s^{-1}) were quantified with a
186 portable thermo-hygrometer (model AK821) at the height of 2.0 m above the soil
187 surface. Soil temperature (T_s, °C) was measured with a portable digital thermometer
188 (model TP101) after each gas flux measurement. Daily precipitation was obtained from
189 an automatic precipitation station installed at a pier on the banks of the Mojuim River in
190 São Caetano das Odivelas (coordinates: -0.738333 latitude; -48.013056 longitude).

191 **2.5   Statistical analyses**

192 On the Macaca Island, two treatments were allocated (low and high topography), with
193 two plots in either treatment. In each plot, eight chambers were randomly distributed,
194 which were considered sample repetitions. The normality of the data of CH_4 and FCO_2
195 flux, and soil physicochemical parameters was evaluated using the Shapiro-Wilks
196 method. The soil CO_2 and CH_4 flux showed a non-normal distribution. Therefore, we
197 used the non-parametric ANOVA (Kruskal-Wallis, $p < 0.05$) to test the differences
198 between the two treatments among months and seasons. The physicochemical
199 parameters were normally distributed. Therefore, a parametric ANOVA was used to test
200 the statistical differences ($p < 0.05$) between the two treatments among months and
201 seasons. Pearson correlation coefficients were calculated to determine the relationships
202 between soil properties and gas fluxes in the months (dry and wet season) when the
203 chemical properties of the soil were analyzed at the same time as gas fluxes were
204 measured. Statistical analyses were performed with the free statistical software Infostat
205 2015®.

3   Results

3.1   Carbon dioxide and methane fluxes

CO_2 fluxes differed significantly between topographies only in January (H = 3.915; p = 0.048), July (H = 9.091; p = 0.003), and November (H = 11.294; p < 0.001) (Figure 2; Supplementary Information, SI 1), with generally higher fluxes at the high topography than at the low topography. At the high topography, CO_2 fluxes were significantly higher (H = 24.510; p = 0.011) in July compared to August and December, March, October, and May, not differing from the other months of the year. Similarly, at the low topography, CO_2 fluxes were statistically higher (H = 19.912; p = 0.046) in September and February than in January and November, not differing from the other months. We found a mean monthly flux of 7.9 ± 0.7 g CO_2 m^{-2} d^{-1} (mean ± standard error) and 5.4 ± 0.5 g CO_2 m^{-2} d^{-1} at the high and low topographies, respectively.
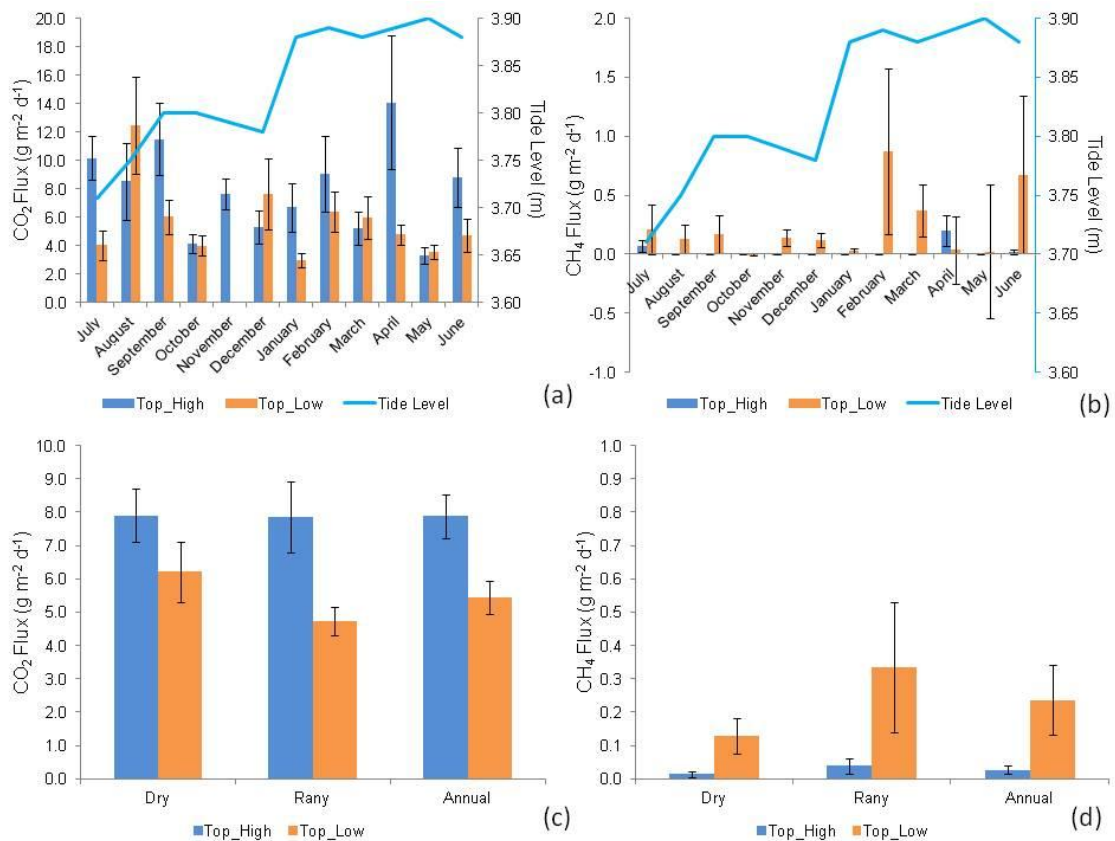
Figure 2. CO_2 (a) and CH_4 (b) fluxes (g CO_2 or CH_4 m^{-2} d^{-1}) monthly (July 2018 to June 2019) (n = 16). Seasonal (Dry and Rainy) and annual fluxes of CO_2 (c) and CH_4 (d), at

222   high (Top_High) and low (Top_Low) topographies (n = 96), in a mangrove forest soil

223   compared to tide level (Tide Level). The bars represent the standard error of the mean.

224   The CH_4 fluxes were statistically different between topographies only in November (H

225   = 9.276; p = 0.002) and December (H = 4.945; p = 0.005), with higher fluxes at the low

226   topography (Figure 2; SI 1). At the high topography, CH_4 fluxes were significantly (H =

227   40.073; p < 0.001) higher in April and July compared to the other months studied, and

228   in November CH_4 was consumed from the atmosphere (Figure 2; SI 1). Similarly, CH_4

229   fluxes at the low topography did not vary significantly among months (H = 10.114; p =

230   0.407).

231   Greenhouse gas fluxes (Figure 2) were only significantly different between

232   topographies in the dry season (Figure 3), period when CO_2 fluxes were higher (H =

233   7.378; p = 0.006) at the high topography and CH_4 fluxes at the low topography (H =

234   8.229; p < 0.001). In the Macaca Island, the mean annual fluxes of CO_2 and CH_4 were

235   6.659 ± 0.419 g CO_2 m^{-2} d^{-1} and 0.132 ± 0.053 g CH_4 m^{-2} d^{-1}, respectively. During the

236   study year, the CO_2 flux from the mangrove soil ranged from -5.06 to 68.96 g CO_2 m^{-2}

237   d^{-1} (mean 6.66 g CO_2 m^{-2} d^{-1}), while the CH_4 flux ranged from -5.07 to 11.08 g CH_4 m^{-2}

238   d^{-1} (mean 0.13 g CH_4 m^{-2} d^{-1}), resulting in a total carbon rate of 1.92 g C m^{-2} d^{-1} or 7.00

239   Mg C ha^{-1} y^{-1} (Figure 2).

240   **3.2   Weather data**

241   There was a marked seasonality during the study period (Figure 2), with 2,155.0 mm of

242   precipitation during the rainy period and 1,016.5 mm during the dry period. The highest

243   tides occurred in the period of greater precipitation (Figure 3) due to the rains. However,

244   the rainfall distribution was different from the climatological normal (Figure 3). The

245   precipitation in the rainy season was 553.2 mm below and in the dry season was 589.1

246   mm above the climatological normal. Thus, in the period studied, the dry season was

247   rainier and the rainy season drier than the climatological normal, which may be a

248   consequence of the La Niña event (Wang et al., 2019).

249

250
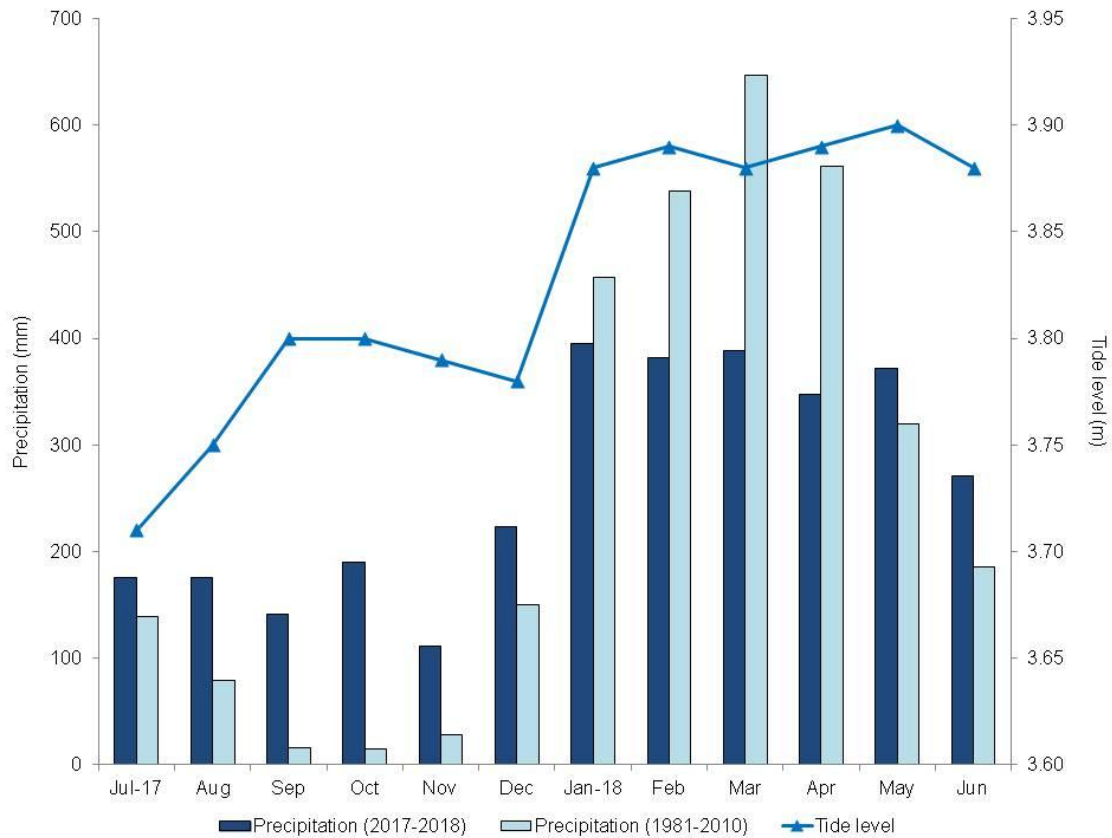
Figure 3. Monthly climatological normal in the municipality of Soure (1981-2010, mm), monthly precipitation (mm), and maximum tide height (m) from 2017 to 2018, in the municipality of São Caetano de Odivelas (PA).

T_{air} was significantly higher (LSD = 0.72, p = 0.01) at the high (31.24 ± 0.26 °C) than at the low topography (30.30 ± 0.25 °C) only in the rainy season (Figure 4a). No significant variation in T_s was found between topographies in either season (Figure 4b). RH was significantly higher (LSD = 2.55, p = 0.01) at the high topography (70.54 ± 0.97%) than at the low topography (66.85 ± 0.87%) only in the rainy season (Figure 4c). W_s (Figure 4d) was significantly higher (LSD = 0.15, p < 0.00) at the low (0.54 ± 0.06 m s^{-1}) than at the high topography (0.24 ± 0.04 m s^{-1}) also in the rainy season.

261
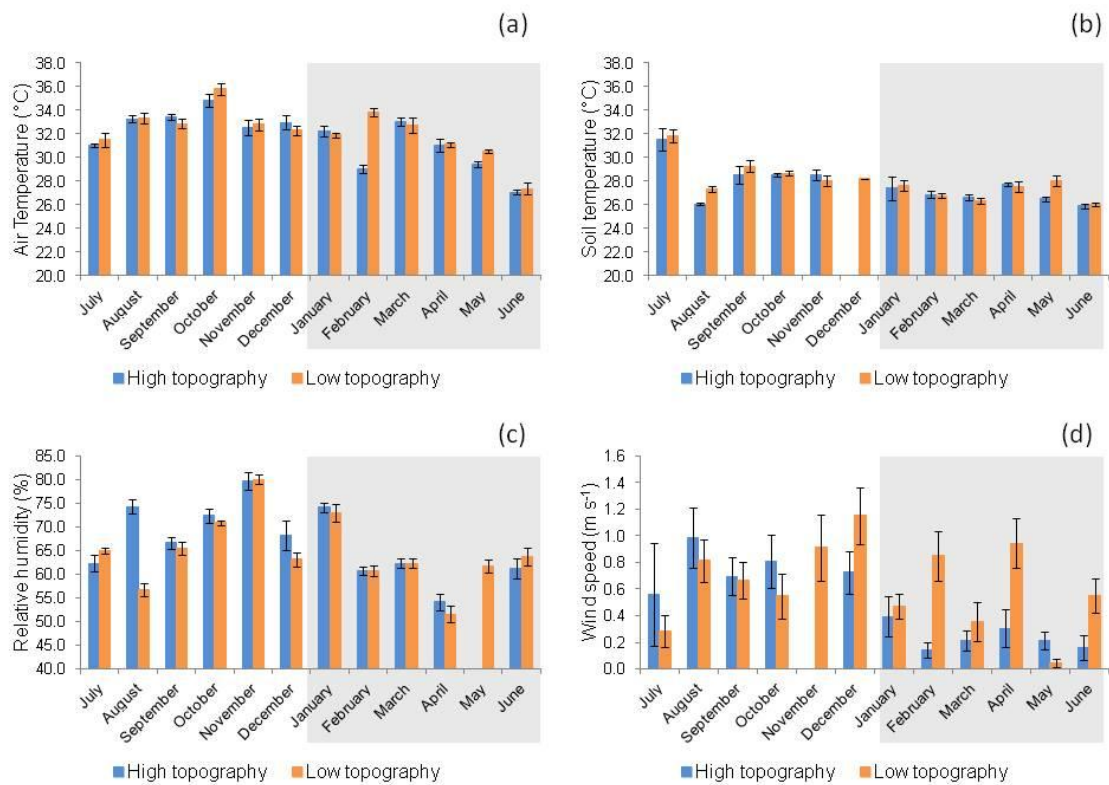
Figure 4. a) Air temperature (°C), b) soil temperature (°C), c) relative humidity (%), and d) wind speed (m s^{-1}) at high and low topographies, from July 2017 to June 2018 in a mangrove area in the Mojuim River estuary. Bars highlighted in grey correspond to the rainy season (n = 16). The bars represent the standard error.

3.3 Soil characteristics

Silt concentration was higher at the low topography (LSD: 14.763; p= 0.007) and clay concentration was higher at the high topography plots (LSD: 12.463; p= 0.005), in both seasons studied (Table 1). Soil particle size analysis did not differ statistically (p > 0.05) between the two seasons (Table 1). Soil moisture did not vary significantly (p > 0.05) between topographies at each season, or between seasonal periods at the same topography (Table 1). The pH varied statistically (LSD: 5.950; p= 0.006) only at the low topography when the two seasons were compared, being more acidic in the dry period (Table 1). The pH values were significantly (LSD: 0.559; p= 0.008) higher in the dry season (Table 1). No variation in Eh was identified between topographies and seasons (Table 1), although it was higher in the dry season than in the rainy season. However, Sal values were higher (LSD: 3.444; p = 0.010) at the high topography than at the low topography in the dry season (Table 1). In addition, Sal was significantly higher

279   in the dry season than in the rainy season, in both high (LSD: 2.916; $p < 0.001$) and low

280   (LSD: 3.003; $p < 0.001$) topographies (Table 1).

Table 1. Analysis of Sand (%), Silt (%), Clay (%), Moisture (%), pH, Redox Potential (Eh, mV) and salinity (Sal; ppt) in the mangrove soil of high and low topographies, and in the rainy and dry seasons (Macaca island, São Caetano das Odivelas). Numbers represent the mean ± standard error of the mean. Lower case letters compare topographies in each seasonal period and upper-case letters compare the same topography between seasonal periods. Different letters indicate statistical difference (LSD, $p < 0.05$).

Season	Topography	Sand (%)	Silt (%)	Clay (%)	Moisture (%)	pH	Eh (mV)	Sal (ppt)
Dry	High	12.1 ± 1.4^{aA}	41.8 ± 3.3^{bA}	46.1 ± 2.6^{aA}	73.1 ± 6.6^{aA}	5.5 ± 0.2^{aA}	190.25 ± 45.53^{aA}	35.25 ± 1.11^{aA}
	Low	9.7 ± 2.5^{aA}	63.6 ± 6.1^{aA}	26.6 ± 5.2^{bA}	86.9 ± 3.4^{aA}	5.3 ± 0.3^{aA}	106.38 ± 53.76^{aA}	30.13 ± 1.16^{bA}
	Mean	10.9 ± 1.4^{A}	52.7 ± 4.4^{A}	36.4 ± 3.8^{A}	80.0 ± 4.0^{A}	5.4 ± 0.2^{A}	148.31 ± 35.71^{A}	32.69 ± 1.02^{A}
Rainy	High	12.1 ± 1.4^{aA}	41.8 ± 3.3^{bA}	46.1 ± 2.6^{aA}	88.9 ± 3.5^{aA}	4.9 ± 0.4^{aA}	92.50 ± 56.20^{aA}	7.50 ± 0.78^{aB}
	Low	9.7 ± 2.5^{aA}	63.6 ± 6.1^{aA}	26.6 ± 5.2^{bA}	88.6 ± 3.7^{aA}	4.4 ± 0.1^{aB}	36.25 ± 49.97^{aA}	8.13 ± 0.79^{aB}
	Mean	10.9 ± 1.4^{A}	52.7 ± 4.4^{A}	36.4 ± 3.8^{A}	88.7 ± 2.5^{A}	4.6 ± 0.2^{B}	64.38 ± 37.04^{A}	7.81 ± 0.54^{B}

286 The C_{mic} did not differ between topographies in the two seasons (Table 2). However, T_C
287 was significantly higher in the low topography in the dry season (LSD: 5.589; p <
288 0.000) and in the rainy season (LSD: 5.777; p = 0.024). In addition, C_{mic} was higher in
289 the dry season in both the high (LSD: 11.325; p < 0.010) and low (LSD: 9.345; p <
290 0.000) topographies (Table 2). N_{mic} did not vary between topographies seasonally.
291 However, N_{mic} in the high (LSD: 9.059; p = 0.013) and low topographies (LSD: 4.447;
292 p = 0.001) was higher during the dry season (Table 2). The C/N ratio (Table 2) was
293 higher in the low than in the high topography in both the dry (LSD: 3.142; p < 0.000)
294 and rainy seasons (LSD: 3.675; p = 0.033). However, only in the low topography was
295 the C/N ratio higher (LSD: 1.863; p < 0.000) in the dry season than in the rainy season
296 (Table 2). Soil OM was higher at the low topography in the rainy (LSD: 9.950; p =
297 0.024) and in the dry seasons (LSD: 9.630; p < 0.000). Only in the lowland topography
298 was the OM concentration higher in the dry season than in the rainy season (Table 2).

299 Table 2. Seasonal and topographic variation in microbial Carbon (C_{mic}; mg kg^{-1}), microbial Nitrogen (N_{mic}, mg kg^{-1}), Total Carbon (T_C; g kg^{-1}),

300 Total Nitrogen (N_T; g kg^{-1}), Carbon/Nitrogen ratio (C/N) and Soil Organic Matter (OM; g kg^{-1}). Numbers represent the mean (±standard error).

301 Lower case letters compare topographies at each season, and upper-case letters compare the topography between seasons.

Season	Topography	C_{mic} mg kg^{-1}	N_{mic} mg kg^{-1}	T_C g kg^{-1}	T_N g kg^{-1}	C/N	OM g kg^{-1}
Dry	High	22.12±5.22^{aA}	12.76±4.20^{aA}	14.12±2.23^{bA}	1.43±0.06^{aA}	9.60±1.20^{bA}	24.35±3.84^{bA}
	Low	26.34±4.23^{aA}	10.34±2.05^{aA}	26.44±1.35^{aA}	1.56±0.04^{aA}	16.98±0.84^{aA}	45.59±2.32^{aA}
	Mean	24.23±3.29^{A}	11.55±2.28^{A}	20.28 ±2.03^{A}	1.49±0.04^{A}	13.29±1.19^{A}	34.97±3.50^{A}
Rainy	High	7.40±0.79^{aB}	0.75±0.41^{aB}	11.46±2.48^{bA}	1.32±0.04^{aA}	8.42±1.70^{bA}	19.75±4.27^{bA}
	Low	5.95±1.06^{aB}	1.23±0.28^{aB}	18.27±1.06^{aB}	1.46±0.06^{aA}	12.47±0.22^{aB}	31.51±1.83^{aB}
	Mean	6.68±0.67^{B}	0.99±0.25^{B}	14.86 ±1.57^{B}	1.39±0.04^{A}	10.44±0.98^{A}	25.63±2.71^{B}

302

3.4 Vegetation structure and biomass

Only the species *R. mangle* and *A. germinans* were found in the floristic survey carried out. The DBH did not vary significantly between the topographies for either species (Table 3). However, *R. mangle* had a higher DBH than *A. germinaris* at both high (LSD: 139.304; $p = 0.037$) and low topographies (LSD: 131.307; $p = 0.001$). The basal area (BA) and AGB did not show significant variation (Table 3). A total aboveground biomass of 322.1 ± 49.6 Mg ha^{-1} was estimated.

311 Table 3: Summed Diameter at Breast Height (DBH; cm), Basal Area (BA; $m^2\,ha^{-1}$) and Aboveground Biomass (AGB; $Mg\,ha^{-1}$) at high and low

312 topographies in the mangrove forest of the Mojuim River estuary. Numbers represent the mean ± standard error of the mean. Lower case letters

313 compare topographic height for each species, and upper-case letters compare species at each topographic height, using Tukey's test ($p < 0.05$).

Specie	Topography	$N\,ha^{-1}$	DBH (cm)	BA ($m^2\,ha^{-1}$)	AGB ($Mg\,ha^{-1}$)
Rhizophora mangle	High	302.4±20.5	238.8±24.9[aA]	17.3±2.0[aA]	219.3±25.7[aA]
	Low	310.4±37.6	283.5±45.0[aA]	24.2±4.3[aA]	338.7±62.9[aA]
Avicennia germinans	High	47.7±20.5	86.8±51.2[aB]	13.8±9.2[aA]	135.3±94.7[aA]
	Low	15.9±9.2	46.1±29.3[aB]	11.8±8.8[aA]	136.0±108.3[aA]
Total	High	350.2±18.4	325.6±33.6[a]	31.1±7.5[a]	304.5±99.8[a]
	Low	346.2±41.0	296.0±23.7[a]	30.0±4.1[a]	330.8±60.4[a]

314 The equations for biomass estimates (AGB) were: *R. mangle* = $0.1282*DBH^{2.6}$; *A. germinans* = $0.14*DBH^{2.4}$; and Total = $0.168*\rho*DBH^{2.47}$, where $\rho_{R.\,mangle}$ = 0.87; $\rho_{A.\,germinans}$

315 = 0.72 (Howard et al., 2014).

316

3.5 Drivers of greenhouse gas fluxes

In the rainy season, CO_2 efflux was correlated with T_{air} (Pearson = 0.23, p = 0.03), RH (Pearson = -0.32, p < 0.00) and T_s (Pearson = 0.21, p = 0.04) only at the low topography. In the dry season CO_2 flux was correlated with T_s (Pearson = 0.39, p < 0.00) at the low topography. The dry season was the period in which we found the greatest amount of significant correlations between CO_2 efflux and soil chemical parameters, while the C:N ratio, OM, and Eh were correlated with CO_2 efflux in both seasons (Table 4). The negative correlation between T_C, N_T, C/N, and OM, along with the positive correlation of N_{mic} with soil CO_2 flux, in the dry period, indicates that microbial activity is a decisive factor for CO_2 efflux (Table 4). Soil moisture in the Mojuim River mangrove forest negatively influenced CO_2 flux in both seasons (Table 4). However, soil moisture was not correlated with CH_4 flux. No significant correlations were found between CH_4 efflux and the chemical properties of the soil in the mangrove of the Mojuim River estuary (Table 4).

331

332 Table 4. Correlation coefficient (Pearson) of CO_2 and CH_4 fluxes with chemical parameters of the soil in a mangrove area in the Mojuim River

333 estuary.

Gas Flux (g m^{-2} d^{-1})	Season	T_C (g kg^{-1})	T_N (g kg^{-1})	C_{mic} (mg kg^{-1})	N_{mic} (mg kg^{-1})	C/N	OM (g kg^{-1})	Sal (ppt)	Eh (mV)	pH	Moisture (%)
CO_2	Dry	-0.68**	-0.59*	0.18^{NS}	0.61**	-0.66**	-0.67**	-0.07^{NS}	0.51*	0.21^{NS}	-0.49*
	Rainy	-0.44^{NS}	-0.20^{NS}	-0.15^{NS}	-0.32^{NS}	-0.50*	-0.63**	-0.54*	0.53*	0.47^{NS}	-0.54*
	Annual	-0.50**	-0.35*	-0.18^{NS}	0.00^{NS}	-0.53**	-0.48**	-0.30^{NS}	0.39*	0.23^{NS}	-0.56**
CH_4	Dry	0.30^{NS}	0.07^{NS}	-0.14^{NS}	-0.24^{NS}	0.34^{NS}	0.02^{NS}	-0.04^{NS}	-0.38^{NS}	0.26^{NS}	0.26^{NS}
	Rainy	0.05^{NS}	-0.09^{NS}	0.44^{NS}	-0.27^{NS}	0.09^{NS}	-0.11^{NS}	-0.04^{NS}	-0.13^{NS}	-0.07^{NS}	0.04^{NS}
	Annual	0.04^{NS}	-0.10^{NS}	-0.01^{NS}	-0.18^{NS}	0.08^{NS}	-0.01^{NS}	-0.17^{NS}	-0.21^{NS}	-0.08^{NS}	0.02^{NS}

334 Total Carbon (T_C; g kg^{-1}); Total Nitrogen (T_N; g kg^{-1}); Microbial Carbon (Cmic, g kg^{-1}); Microbial Nitrogen (N_{mic}, g kg^{-1}); Carbon and Nitrogen

335 ratio (C/N); Organic Matter (OM; g kg^{-1}); Salinity (Sal; ppt); Redox Potential (Eh; mV); Soil Moisture (Moisture, %).

336 NS= not significant; * significant effects at $p \leq 0.05$; ** significant effects at $p \leq 0.01$

337

4   Discussion

4.1   Carbon dioxide and methane flux

It is important to consider that the year under study was rainier in the dry season (2017) and less rainy in the wet season (2018) when the climatological average is concerned (1981-2010) (Figure 3). Perhaps this variation is related to the effects of global climate changes. Under these conditions, negative and positive fluxes of the two greenhouse gases were found (negative values represent gas consumption). The negative CO_2 flux is apparently a consequence of the increased CO_2 solubility in tidal waters or of the increased sulfate reduction, as described in the literature (Borges et al., 2018; Chowdhury et al., 2018; Nóbrega et al., 2016). Fluctuations in redox potential altered the availability of the terminal electron acceptor and donor, and the forces of recovery of their concentrations in the soil, such that a disproportionate release of CO_2 can result from the alternative anaerobic degradation processes such as sulfate and iron reduction (Chowdhury et al., 2018). The soil carbon flux in the mangrove area in the Amazon region was within the range of findings for other tropical mangrove areas (2.6 to 11.0 g CO_2 m^{-2} d^{-1}; Shiau and Chiu, 2020). However, the mean flux of 6.2 mmol CO_2 m^{-2} h^{-1} recorded in this Amazonian mangrove was much higher than the mean efflux of 2.9 mmol CO_2 m^{-2} h^{-1} recorded in 75 mangroves during low tide periods (Alongi, 2009).

An emission of 0.01 Tg CH_4 y^{-1}, 0.6 g CH_4 m^{-2} d^{-1} (Rosentreter et al., 2018a), or 26.7 mg CH_4 m^{-2} h^{-1} has been reported for tropical latitudes (0 and 5°). In our study, the monthly average of CH_4 flux was higher at the low (7.3 ± 8.0 mg CH_4 m^{-2} h^{-1}) than at the high topography (0.9 ± 0.6 mg C m^{-2} h^{-1}), resulting in 0.1 g CH_4 m^{-2} d^{-1} or 0.5 Mg CH_4 ha^{-1} y^{-1} (Figure 2). Therefore, the CH_4-C fluxes from the mangrove soil in the Mojuim River estuary were much lower than expected. It is known that there is a microbial functional module for CH_4 production and consumption (Xu et al., 2015) and diffusibility of CH_4 (Sihi et al., 2018), and this module considers three key mechanisms: aceticlastic methanogenesis (acetate production), hydrogenotrophic methanogenesis (H_2 and CO_2 production), and aerobic methanotrophy (CH_4 oxidation and O_2 reduction). The average emission from the soil of 8.4 mmol CH_4 m^{-2} d^{-1} was well below the fluxes recorded in the Bay of Bengal, with 18.4 mmol CH_4 m^{-2} d^{-1} (Biswas et al., 2007). In the Amazonian mangrove studied the mean annual carbon equivalent efflux was 429.6 mg $CO_{2\text{-eq}}$ m^{-2} h^{-1}. This value is insignificant compared to the projected erosion losses of 103.5 Tg $CO_{2\text{-eq}}$ ha^{-1} y^{-1} for the next century in tropical mangrove forests (Adame et al.,

371 2021). These higher CO_2 flux concomitantly with lower CH_4 flux in this Amazonian

372 estuary are probably a consequence of changes in the rainfall pattern already underway,

373 where the dry season was wetter and the rainy season drier when compared to the

374 climatological normal. The most recent estimate between latitude 0° to 23.5° S shows

375 an emission of 2.3 g CO_2 m^{-2} d^{-1} (Rosentreter et al., 2018b). However, the efflux in the

376 mangrove of the Mojuim River estuary was 6.7 g CO_2 m^{-2} d^{-1}. For the same latitudinal

377 range, Rosentreter et al. (2018c) estimated an emission of 0.6 g CH_4 m^{-2} d^{-1}, and we

378 found an efflux of 0.1 g CH_4 m^{-2} d^{-1}.

379 **4.2   Drivers of greenhouse gas fluxes**

380 Mangrove areas are periodically flooded, with a larger flood volume during the syzygy

381 tides, especially in the rainy season. The hydrological condition of the soil is determined

382 by the microtopography and can regulate the respiration of microorganisms (aerobic or

383 anaerobic), being a decisive factor in controlling the CO_2 efflux (Dai et al., 2012;

384 Davidson et al., 2000; Ehrenfeld, 1995). No significant influence on CO_2 flux was

385 observed due to the low variation in high tide level throughout the year (0.19 m) (Figure

386 2), although it was numerically higher at the high topography. However, tidal height

387 and the rainy season resulted in a higher CO_2 flux (rate high/low =1.7) at the high

388 topography (7.86 ± 0.04 g CO_2 m^{-2} d^{-1}) than at the low topography (4.73 ± 0.34 g CO_2

389 m^{-2} d^{-1}) (Figure 2; SI 1). This result may be due to the root systems of most flood-

390 tolerant plants remaining active when flooded (Angelov et al., 1996). Still, the high

391 topography has longer flood-free periods, which only happens when the tides are

392 syzygy or when the rains are torrential.

393 CO_2 efflux was higher in the high topography than in the low topography in the rainy

394 season (when soils are more subject to inundation), i.e., 39.8% lower in the forest soil

395 exposed to the atmosphere for less time. Measurements performed on 62 mangrove

396 forest soils showed an average flux of 2.87 mmol CO_2 m^{-2} h^{-1} when the soil was

397 exposed to the atmosphere, while 75 results on flooded mangrove forest soils showed an

398 average emission of 2.06 mmol CO_2 m^{-2} h^{-1} (Alongi, 2007, 2009), i.e., 28.2% less than

399 for the dry soil. This reflects the increased facility gases have for molecular diffusion

400 than fluids, and the increased surface area available for aerobic respiration and chemical

401 oxidation during air exposure (Chen et al., 2010). Some studies attribute this variation

402 to the temperature of the soil when it is exposed to tropical air (Alongi, 2009), which

403 increases the export of dissolved inorganic carbon (Maher et al., 2018). However,

although despite the lack of significant variation in soil temperature between topographies at each time of year (Figure 4b), there was a positive correlation (Pearson = 0.15, p = 0.05) between CO_2 efflux and soil temperature at the low topography.

Some studies show that CH_4 efflux is a consequence of the seasonal temperature variation in mangrove forest under temperate/monsoon climates (Chauhan et al., 2015; Purvaja and Ramesh, 2001; Whalen, 2005). However, in your study CH_4 efflux was correlated with Ta (Pearson = -0.33, p < 0.00) and RH (Pearson = 0.28, p = 0.01) only in the dry season and at the low topography. The results show that the physical parameters do not affect the fluxes in a standardized way, and their greater or lesser influence depends on the topography and seasonality.

A compilation of several studies showed that the total CH_4 emissions from the soil in a mangrove ecosystem range from 0 to 23.68 mg C m^{-2} h^{-1} (Shiau and Chiu, 2020), and our study showed a range of -0.01 to 31.88 mg C m^{-2} h^{-1} (mean of 4.70 ± 5.00 mg C m^{-2} h^{-1}). The monthly CH_4 fluxes were generally higher at the low (0.232 ± 0.256 g CH_4 m^{-2} d^{-1}) than at the high (0.026 ± 0.018 g CH_4 m^{-2} d^{-1}) topography, especially during the rainy season when the tides were higher (Figure 2). Only in the dry season was there a significantly higher production at the low than at the high topography (Figure 2; SI 1). The low topography produced 0.0249 g C m^{-2} h^{-1} more to the atmosphere in the rainy season than in the dry season (Figure 2), and a similar seasonal pattern was recorded in other studies (Cameron et al., 2021).

The mangrove soil in the Mojuim River estuary is rich in silt and clay (Table 1), which reduces sediment porosity and fosters the formation and maintenance of anoxic conditions (Dutta et al., 2013). In addition, the lack of oxygen in the flooded mangrove soil favors microbial processes such as denitrification, sulfate reduction, methanogenesis, and redox reactions (Alongi and Christoffersen, 1992). A significant amount of CH_4 produced in wetlands is dissolved in the pore water due to high pressure, causing supersaturation, which allows CH_4 to be released by diffusion from the sediment to the atmosphere and by boiling through the formation of bubbles.

Studies show that the CO_2 flux tends to be lower with high soil saturation (Chanda et al., 2014; Kristensen et al., 2008). A total of 395 Mg C ha^{-1} was found at the soil surface (0.15 m) in the mangrove of the Mojuim River estuary, which was slightly higher than the 340 Mg C ha^{-1} found in other mangroves in the Amazon (Kauffman et al., 2018), however being significantly 1.8 times greater at the low topography (Table 2). The finer

437   soil texture at the low topography (Table 1) reduces groundwater drainage which

438   facilitates the accumulation of C in the soil (Schmidt et al., 2011).

4.3   Mangrove biomass

440   Only the species *R. mangle* and *A. germinans* were found in the floristic survey carried

441   out, which is aligned with the results of other studies in the same region (Menezes et al.,

442   2008). Thus, the variations found in the flux between the topographies in the Mojuim

443   River estuary are not related to the mangrove forest structure, because there was no

444   difference in the aboveground biomass. Since there was no difference in the species

445   composition, the belowground biomass is not expected to differ either (Table 3).

446   Assuming that the amount of carbon stored is 42.0% of the total biomass (Sahu and

447   Kathiresan, 2019), the mangrove forest biomass of the Mojuim River estuary stores

448   127.9 and 138.9 Mg C ha^{-1} at the high and low topographies, respectively. This result is

449   lower than the 507.8 Mg C ha^{-1} estimated for Brazilian mangroves (Hamilton and

450   Friess, 2018), but are near the 103.7 Mg C ha^{-1} estimated for a mangrove at Guará's

451   island (Salum et al., 2020), 108.4 Mg C ha^{-1} for the Bragantina region (Gardunho,

452   2017), and 132.3 Mg C ha^{-1} in French Guiana (Fromard et al., 1998). Thus, the biomass

453   found in the Mojuim estuary does not differ from the biomass found in other

454   Amazonian mangroves. The estimated primary production for tropical mangrove forests

455   is 218 ± 72 Tg C y^{-1} (Bouillon et al., 2008).

4.4   Biogeochemical parameters

457   During the seasonal and annual periods, CH_4 efflux was not significantly correlated

458   with chemical parameters (Table 5), which is similar to the observed in another study

459   (Chen et al., 2010). Flooded soils present reduced gas diffusion rates, which directly

460   affects the physiological state and activity of microbes, by limiting the supply of the

461   dominant electron acceptors (e.g., oxygen), and gases (e.g., CH_4) (Blagodatsky and

462   Smith, 2012). The importance of soil can be reflected in bacterial richness and diversity

463   compared to pore spaces filled with water (Banerjee et al., 2016). On the other hand,

464   increasing soil moisture provides the microorganisms with essential substrates such as

465   ammonium, nitrate, and soluble organic carbon, and increases gas diffusion rates in the

466   water (Blagodatsky and Smith, 2012). Biologically available nitrogen often limit marine

467   productivity (Bertics et al., 2010), and thus can affect CO_2 fluxes to the atmosphere.

468   However, a mangrove fertilization experiment showed that CH_4 emission rates were not

469 affected by N addition (Kreuzwieser et al., 2003). A higher concentration of C_{mic} and
470 N_{mic} in the dry period (Table 2), both in the high and low topographies, indicated that
471 microorganisms are more active when the soil spends more time aerated in the dry
472 period (Table 2), time when only the high tides produce anoxia in the mangrove soil
473 mainly in the low topography. Under reduced oxygen conditions, in a laboratory
474 incubated mangrove soil, the addition of nitrogen resulted in a significant increase in the
475 microbial metabolic quotient, showing no concomitant change in microbial respiration,
476 which was explained by a decrease in microbial biomass (Craig et al., 2021).

477 The high OM concentration at the two topographic locations (Table 2), at the two
478 seasons studied, and the respective negative correlation with CO_2 flux (Table 5) confirm
479 the importance of microbial activity in mangrove soils (Gao et al., 2020). Also, CH_4
480 produced in flooded soils can be converted mainly to CO_2 by the anaerobic oxidation of
481 CH_4 (Boetius et al., 2000; Milucka et al., 2015; Xu et al., 2015) which may contribute to
482 the higher CO_2 efflux in the Mojuim River estuary compared to other tropical
483 mangroves (Rosentreter et al., 2018b). The belowground C stock is considered the
484 largest C reservoir in a mangrove ecosystem, and it results from the low OM
485 decomposition rate due to flooding (Marchand, 2017).

486 The higher water salinity influenced by the tidal movement in the dry season (Table 1)
487 seems to result in a lower CH_4 flux at the low topography (Dutta et al., 2013; Lekphet et
488 al., 2005; Shiau and Chiu, 2020). High SO_4^{2-} concentration in the marine sediments
489 inhibits methane formation due to competition between SO_4^{2-} reduction and
490 methanogenic fermentation, as sulfate-reducing bacteria are more efficient at using
491 hydrogen than methanotrophic bacteria (Abram and Nedwell, 1978; Kristjansson et al.,
492 1982), a key factor fostering reduced CH_4 emissions. At high SO_4^{2-} concentrations
493 methanotrophic bacteria use CH_4 as an energy source and oxidize it to CO_2 (Coyne,
494 1999; Segarra et al., 2015), increasing the efflux of CO_2 and reduced CH_4 (Megonigal
495 and Schlesinger, 2002; Roslev and King, 1996). This may explain the high CO_2 and low
496 CH_4 efflux found throughout the year at the high and, especially, at the low
497 topographies (Figure 3).

498 Studies in coastal ecosystems in Taiwan have reported that methanotrophic bacteria can
499 be sensitive to soil pH, and reported an optimal growth at pH ranging from 6.5 to 7.5
500 (Shiau et al., 2018). The higher soil acidity in the Mojuim River wetland (Table 1) may
501 be inhibiting the activity of methanogenic bacteria by increasing the population of

502   methanotrophic bacteria, which are efficient in CH_4 consumption (Chen et al., 2010;

503   Hegde et al., 2003; Shiau and Chiu, 2020). In addition, the pneumatophores present in

504   *R. mangle* increase soil aeration and reduce CH_4 emissions (Allen et al., 2011; He et al.,

505   2019). Spatial differences (topography) in CH_4 emissions in the soil can be attributed to

506   substrate heterogeneity, salinity, and the abundance of methanogenic and

507   methanotrophic bacteria (Gao et al., 2020). Increases in CH_4 efflux with reduced

508   salinity were found as a consequence of intense oxidation or reduced competition from

509   the more energetically efficient SO_4^{2-} and NO^{3-} reducing bacteria when compared to the

510   methanogenic bacteria (Biswas et al., 2007). This fact can be observed in the CH_4 efflux

511   in the mangrove of the Mojuim River, because there was an increased CH_4 production

512   especially in the low topography in the rainy season (Figure 3), when water salinity is

513   reduced (Table 1) due to the increased precipitation. However, we did not find a

514   correlation between CH_4 efflux and salinity, as previously reported (Purvaja and

515   Ramesh, 2001). More detailed studies on CH_4 efflux and on its relationship with

516   methanotrophic bacteria and abiotic factors (mainly ammonia and sulfate) are needed

517   due to the average flux of 4.70 mg C m^{-2} h^{-1} and the extreme monthly and seasonal

518   variations.

5   Conclusions

520   Seasonality was important for CH_4 efflux but did not influence CO_2 efflux. The

521   differences in fluxes may be an effect of global climate changes on the terrestrial

522   biogeochemistry at the plant-soil-atmosphere interface, as indicated by the deviation in

523   precipitation values from the climatology normal, making it necessary to extend this

524   study for more years. Using the factor of 23 to convert the global warming potential of

525   CH_4 to CO_2 (IPCC, 2001), the CO_2 equivalent emission was 35.4 Mg CO_{2-eq} ha^{-1} yr^{-1}.

526   Over a 100-year time period, a radiative forcing due to the continuous emission of 0.05

527   kg CH_4 m^{-2} y^{-1}found in this study, would be offset if CO_2 sequestration rates were 2.16

528   kg CO_2 m^{-2} y^{-1} (Neubauer and Megonigal, 2015).

529   Microtopography should be considered when determining the efflux of CO_2 and CH_4 in

530   mangrove forests in an Amazon estuary. The low topography in the mangrove forest of

531   Mojuim River had a higher concentration of organic carbon in the soil. However, it did

532   not produce a higher CO_2 efflux because it was negatively influenced by soil moisture,

533   which was indifferent to CH_4 efflux. MO, C/N ratio, and Eh were critical in soil

534   microbial activity, which resulted in a variation in CO_2 flux during the year and

535 seasonal periods. Thus, the physicochemical properties of the soil are important for CO_2

536 flux, especially in the rainy season. Still, they did not influence CH_4 fluxes.

537 *Data availability*: The data used in this article belong to the doctoral thesis of Saul

538 Castellón, within the Postgraduate Program in Environmental Sciences, at the Federal

539 University of Pará. Access to the data can be requested from Dr. Castellón

540 (saulmarz22@gmail.com), which holds the set of all data used in this paper.

541 *Author contributions:* SEMC and JHC designed the study and wrote the article with the

542 help of JFB, MR, MLR, and CN. JFB assisted in the field experiment. MR provided

543 logistical support in field activities.

544 *Competing interests*: The authors declare that they have no conflict of interest

545 *Acknowledgements*: The authors are grateful to the Program of Alliances for Education

546 and Training of the Organization of the American States and to Coimbra Group of

547 Brazilian Universities, for the financial support, as well as to Paulo Sarmento for the

548 assistance at laboratory analysis, and to Maridalva Ribeiro and Lucivaldo da Silva for

549 the fieldwork assistance. Furthermore, the authors would like to thank the Laboratory of

550 Biogeochemical Cycles (Geosciences Institute, Federal University of Pará) for the

551 equipment provided for this research.

6   References

553 Abram, J. W. and Nedwell, D. B.: Inhibition of methanogenesis by sulphate reducing

554 bacteria competing for transferred hydrogen, Arch. Microbiol., 117(1), 89–92,

555 doi:10.1007/BF00689356, 1978.

556 Adame, M. F., Connolly, R. M., Turschwell, M. P., Lovelock, C. E., Fatoyinbo, T.,

557 Lagomasino, D., Goldberg, L. A., Holdorf, J., Friess, D. A., Sasmito, S. D., Sanderman,

558 J., Sievers, M., Buelow, C., Kauffman, J. B., Bryan-Brown, D. and Brown, C. J.: Future

559 carbon emissions from global mangrove forest loss, Glob. Chang. Biol., 27(12), 2856–

560 2866, doi:10.1111/gcb.15571, 2021.

561 Allen, D., Dalal, R. C., Rennenberg, H. and Schmidt, S.: Seasonal variation in nitrous

562 oxide and methane emissions from subtropical estuary and coastal mangrove sediments,

563 Australia, Plant Biol., 13(1), 126–133, doi:10.1111/j.1438-8677.2010.00331.x, 2011.

564 Almeida, R. F. de, Mikhael, J. E. R., Franco, F. O., Santana, L. M. F. and Wendling, B.:

565 Measuring the labile and recalcitrant pools of carbon and nitrogen in forested and

agricultural soils: A study under tropical conditions, Forests, 10(7), 544, doi:10.3390/f10070544, 2019.

Alongi, D. M.: The contribution of mangrove ecosystems to global carbon cycling and greenhouse gas emissions, in Greenhouse gas and carbon balances in mangrove coastal ecosystems, edited by Y. Tateda, R. Upstill-Goddard, T. Goreau, D. M. Alongi, A. Nose, E. Kristensen, and G. Wattayakorn, pp. 1–10, Gendai Tosho, Kanagawa, Japan., 2007.

Alongi, D. M.: The Energetics of Mangrove Forests, Springer Netherlands, Dordrecht., 2009.

Alongi, D. M. and Christoffersen, P.: Benthic infauna and organism-sediment relations in a shallow, tropical coastal area: influence of outwelled mangrove detritus and physical disturbance, Mar. Ecol. Prog. Ser., 81(3), 229–245, doi:10.3354/meps081229, 1992.

Alongi, D. M. and Mukhopadhyay, S. K.: Contribution of mangroves to coastal carbon cycling in low latitude seas, Agric. For. Meteorol., 213, 266–272, doi:10.1016/j.agrformet.2014.10.005, 2015.

Angelov, M. N., Sung, S. J. S., Doong, R. Lou, Harms, W. R., Kormanik, P. P. and Black, C. C.: Long-and short-term flooding effects on survival and sink-source relationships of swamp-adapted tree species, Tree Physiol., 16(4), 477–484, doi:10.1093/treephys/16.5.477, 1996.

Araujo, A. S. F. de: Is the microwave irradiation a suitable method for measuring soil microbial biomass?, Rev. Environ. Sci. Biotechnol., 9(4), 317–321, doi:10.1007/s11157-010-9210-y, 2010.

Banerjee, S., Helgason, B., Wang, L., Winsley, T., Ferrari, B. C. and Siciliano, S. D.: Legacy effects of soil moisture on microbial community structure and N2O emissions, Soil Biol. Biochem., 95, 40–50, doi:10.1016/j.soilbio.2015.12.004, 2016.

Bastviken, D., Tranvik, L. J., Downing, J. A., Crill, P. M. and Enrich-Prast, A.: Freshwater Methane Emissions Offset the Continental Carbon Sink, Science (80-.)., 331(6013), 50–50, doi:10.1126/science.1196808, 2011.

Bauza, J. F., Morell, J. M. and Corredor, J. E.: Biogeochemistry of Nitrous Oxide Production in the Red Mangrove (Rhizophora mangle) Forest Sediments, Estuar. Coast.

597   Shelf Sci., 55(5), 697–704, doi:10.1006/ECSS.2001.0913, 2002.

598   Bertics, V. J., Sohm, J. A., Treude, T., Chow, C. E. T., Capone, D. G., Fuhrman, J. A.
599   and Ziebis, W.: Burrowing deeper into benthic nitrogen cycling: The impact of
600   Bioturbation on nitrogen fixation coupled to sulfate reduction, Mar. Ecol. Prog. Ser.,
601   409, 1–15, doi:10.3354/meps08639, 2010.

602   Biswas, H., Mukhopadhyay, S. K., Sen, S. and Jana, T. K.: Spatial and temporal
603   patterns of methane dynamics in the tropical mangrove dominated estuary, NE coast of
604   Bay of Bengal, India, J. Mar. Syst., 68(1–2), 55–64, doi:10.1016/j.jmarsys.2006.11.001,
605   2007.

606   Blagodatsky, S. and Smith, P.: Soil physics meets soil biology: Towards better
607   mechanistic prediction of greenhouse gas emissions from soil, Soil Biol. Biochem., 47,
608   78–92, doi:10.1016/J.SOILBIO.2011.12.015, 2012.

609   Boetius, A., Ravenschlag, K., Schubert, C. J., Rickert, D., Widdel, F., Gleseke, A.,
610   Amann, R., Jørgensen, B. B., Witte, U. and Pfannkuche, O.: A marine microbial
611   consortium apparently mediating anaerobic oxidation methane, Nature, 407(6804), 623–
612   626, doi:10.1038/35036572, 2000.

613   Borges, A. V., Abril, G., Darchambeau, F., Teodoru, C. R., Deborde, J., Vidal, L. O.,
614   Lambert, T. and Bouillon, S.: Divergent biophysical controls of aquatic CO_2 and CH_4
615   in the World's two largest rivers, Sci. Rep., 5, doi:10.1038/srep15614, 2015.

616   Borges, A. V., Abril, G. and Bouillon, S.: Carbon dynamics and CO_2 and CH_4
617   outgassing in the Mekong delta, Biogeosciences, 15(4), 1093–1114, doi:10.5194/bg-15-
618   1093-2018, 2018.

619   Bouillon, S., Borges, A. V., Castañeda-Moya, E., Diele, K., Dittmar, T., Duke, N. C.,
620   Kristensen, E., Lee, S. Y., Marchand, C., Middelburg, J. J., Rivera-Monroy, V. H.,
621   Smith, T. J. and Twilley, R. R.: Mangrove production and carbon sinks: A revision of
622   global   budget   estimates,   Global   Biogeochem.   Cycles,   22(2),   1–12,
623   doi:10.1029/2007GB003052, 2008.

624   Brookes, P. C., Landman, A., Pruden, G. and Jenkinson, D. S.: Chloroform fumigation
625   and the release of soil nitrogen: A rapid direct extraction method to measure microbial
626   biomass nitrogen in soil, Soil Biol. Biochem., 17(6), 837–842, doi:10.1016/0038-
627   0717(85)90144-0, 1985.

628 Cameron, C., Hutley, L. B., Munksgaard, N. C., Phan, S., Aung, T., Thinn, T., Aye, W.

629 M. and Lovelock, C. E.: Impact of an extreme monsoon on CO_2 and CH_4 fluxes from

630 mangrove soils of the Ayeyarwady Delta, Myanmar, Sci. Total Environ., 760, 143422,

631 doi:10.1016/j.scitotenv.2020.143422, 2021.

632 Castillo, J. A. A., Apan, A. A., Maraseni, T. N. and Salmo, S. G.: Soil greenhouse gas

633 fluxes in tropical mangrove forests and in land uses on deforested mangrove lands,

634 Catena, 159, 60–69, doi:10.1016/j.catena.2017.08.005, 2017.

635 Chanda, A., Akhand, A., Manna, S., Dutta, S., Das, I., Hazra, S., Rao, K. H. and

636 Dadhwal, V. K.: Measuring daytime CO_2 fluxes from the inter-tidal mangrove soils of

637 Indian Sundarbans, Environ. Earth Sci., 72(2), 417–427, doi:10.1007/s12665-013-2962-

638 2, 2014.

639 Chauhan, R., Datta, A., Ramanathan, A. and Adhya, T. K.: Factors influencing spatio-

640 temporal variation of methane and nitrous oxide emission from a tropical mangrove of

641 eastern   coast   of   India,   Atmos.   Environ.,   107,   95–106,

642 doi:10.1016/j.atmosenv.2015.02.006, 2015.

643 Chen, G. C., Tam, N. F. Y. and Ye, Y.: Spatial and seasonal variations of atmospheric

644 N_2O and CO_2 fluxes from a subtropical mangrove swamp and their relationships with

645 soil   characteristics,   Soil   Biol.   Biochem.,   48,   175–181,

646 doi:10.1016/j.soilbio.2012.01.029, 2012.

647 Chen, G. C., Ulumuddin, Y. I., Pramudji, S., Chen, S. Y., Chen, B., Ye, Y., Ou, D. Y.,

648 Ma, Z. Y., Huang, H. and Wang, J. K.: Rich soil carbon and nitrogen but low

649 atmospheric greenhouse gas fluxes from North Sulawesi mangrove swamps in

650 Indonesia, Sci. Total Environ., 487(1), 91–96, doi:10.1016/j.scitotenv.2014.03.140,

651 2014.

652 Chen, G. C. C., Tam, N. F. Y. F. Y. and Ye, Y.: Summer fluxes of atmospheric

653 greenhouse gases N_2O, CH_4 and CO_2 from mangrove soil in South China, Sci. Total

654 Environ., 408(13), 2761–2767, doi:10.1016/j.scitotenv.2010.03.007, 2010.

655 Chowdhury, T. R., Bramer, L., Hoyt, D. W., Kim, Y. M., Metz, T. O., McCue, L. A.,

656 Diefenderfer, H. L., Jansson, J. K. and Bailey, V.: Temporal dynamics of CO_2 and CH_4

657 loss potentials in response to rapid hydrological shifts in tidal freshwater wetland soils,

658 Ecol. Eng., 114, 104–114, doi:10.1016/j.ecoleng.2017.06.041, 2018.

659   Chuang, P. C., Young, M. B., Dale, A. W., Miller, L. G., Herrera-Silveira, J. A. and
660   Paytan, A.: Methane and sulfate dynamics in sediments from mangrove-dominated
661   tropical coastal lagoons, Yucatan, Mexico, Biogeosciences, 13(10), 2981–3001, 2016.

662   Coyne, M.: Soil Microbiology: An Exploratory Approach, Delmar Publishers, New
663   York, NY, USA., 1999.

664   Craig, H., Antwis, R. E., Cordero, I., Ashworth, D., Robinson, C. H., Osborne, T. Z.,
665   Bardgett, R. D., Rowntree, J. K. and Simpson, L. T.: Nitrogen addition alters
666   composition, diversity, and functioning of microbial communities in mangrove soils:
667   An incubation experiment, Soil Biol. Biochem., 153, 108076,
668   doi:10.1016/j.soilbio.2020.108076, 2021.

669   Dai, Z., Trettin, C. C., Li, C., Li, H., Sun, G. and Amatya, D. M.: Effect of Assessment
670   Scale on Spatial and Temporal Variations in CH4, CO2, and N2O Fluxes in a Forested
671   Wetland, Water, Air, Soil Pollut., 223(1), 253–265, doi:10.1007/s11270-011-0855-0,
672   2012.

673   Davidson, E. A., Verchot, L. V., Cattanio, J. H., Ackerman, I. L. and Carvalho, J. E. M.:
674   Effects of soil water content on soil respiration in forests and cattle pastures of eastern
675   Amazonia, Biogeochemistry, 48(1), 53–69, doi:10.1023/a:1006204113917, 2000.

676   Donato, D. C., Kauffman, J. B., Murdiyarso, D., Kurnianto, S., Stidham, M. and
677   Kanninen, M.: Mangroves among the most carbon-rich forests in the tropics, Nat.
678   Geosci., 4(5), 293–297, doi:10.1038/ngeo1123, 2011.

679   Dutta, M. K., Chowdhury, C., Jana, T. K. and Mukhopadhyay, S. K.: Dynamics and
680   exchange fluxes of methane in the estuarine mangrove environment of the Sundarbans,
681   NE coast of India, Atmos. Environ., 77, 631–639, doi:10.1016/j.atmosenv.2013.05.050,
682   2013.

683   Ehrenfeld, J. G.: Microsite differences in surface substrate characteristics in
684   Chamaecyparis swamps of the New Jersey Pinelands, Wetlands, 15(2), 183–189,
685   doi:10.1007/BF03160672, 1995.

686   El-Robrini, M., Alves, M. A. M. S., Souza Filho, P. W. M., El-Robrini M. H. S., Silva
687   Júnior, O. G. and França, C. F.: Atlas de Erosão e Progradação da zona costeira do
688   Estado do Pará – Região Amazônica: Áreas oceânica e estuarina, in Atlas de Erosão e
689   Progradação da Zona Costeira Brasileira, edited by D. Muehe, pp. 1–34, São Paulo.,

690 2006.

691 EPA, E. P. A.: Inventory of U.S. Greenhouse Gas Emissions and Sinks: 1990–2015.,
692 2017.

693 Fernandes, W. A. A. and Pimentel, M. A. da S.: Dinâmica da paisagem no entorno da
694 RESEX marinha de São João da Ponta/PA: utilização de métricas e geoprocessamento,
695 Caminhos Geogr., 20(72), 326–344, doi:10.14393/RCG207247140, 2019.

696 Ferreira, A. S., Camargo, F. A. O. and Vidor, C.: Utilização de microondas na avaliação
697 da biomassa microbiana do solo, Rev. Bras. Ciência do Solo, 23(4), 991–996,
698 doi:10.1590/S0100-06831999000400026, 1999.

699 Ferreira, S. da S.: Entre marés e mangues: paisagens territorializadas por pescadores da
700 resex marinha de São João da Ponta (PA), Federal University of Pará., 2017.

701 França, C. F. de, Pimentel, M. A. D. S. and Neves, S. C. R.: Estrutura Paisagística De
702 São João Da Ponta, Nordeste Do Pará, Geogr. Ensino Pesqui., 20(1), 130–142,
703 doi:10.5902/2236499418331, 2016.

704 Frankignoulle, M.: Field measurements of air-sea CO2 exchange, Limnol. Oceanogr.,
705 33(3), 313–322, 1988.

706 Friesen, S. D., Dunn, C. and Freeman, C.: Decomposition as a regulator of carbon
707 accretion   in   mangroves: a   review,   Ecol.   Eng.,   114,   173–178,
708 doi:10.1016/j.ecoleng.2017.06.069, 2018.

709 Fromard, F., Puig, H., Cadamuro, L., Marty, G., Betoulle, J. L. and Mougin, E.:
710 Structure, above-ground biomass and dynamics of mangrove ecosystems: new data
711 from French Guiana, Oecologia, 115(1), 39–53, doi:10.1007/s004420050489, 1998.

712 Gao, G. F., Zhang, X. M., Li, P. F., Simon, M., Shen, Z. J., Chen, J., Gao, C. H. and
713 Zheng, H. L.: Examining Soil Carbon Gas (CO2, CH4) Emissions and the Effect on
714 Functional Microbial Abundances in the Zhangjiang Estuary Mangrove Reserve, J.
715 Coast. Res., 36(1), 54–62, doi:10.2112/JCOASTRES-D-18-00107.1, 2020.

716 Gardunho, D. C. L.: Estimativas de biomassa acima do solo da floresta de mangue na
717 península de Ajuruteua, Bragança – PA, Federal University of Pará, Belém, Brazil.,
718 2017.

719 Hamilton, S. E. and Friess, D. A.: Global carbon stocks and potential emissions due to

720   mangrove deforestation from 2000 to 2012, Nat. Clim. Chang., 8(3), 240–244,
721   doi:10.1038/s41558-018-0090-4, 2018.

722   He, Y., Guan, W., Xue, D., Liu, L., Peng, C., Liao, B., Hu, J., Zhu, Q., Yang, Y., Wang,
723   X., Zhou, G., Wu, Z. and Chen, H.: Comparison of methane emissions among invasive
724   and native mangrove species in Dongzhaigang, Hainan Island, Sci. Total Environ., 697,
725   133945, doi:10.1016/j.scitotenv.2019.133945, 2019.

726   Hegde, U., Chang, T.-C. and Yang, S.-S.: Methane and carbon dioxide emissions from
727   Shan-Chu-Ku landfill site in northern Taiwan., Chemosphere, 52(8), 1275–1285,
728   doi:10.1016/S0045-6535(03)00352-7, 2003.

729   Herz, R.: Manguezais do Brasil, Instituto Oceanografico da USP/CIRM, São Paulo,
730   Brazil., 1991.

731   Howard, J., Hoyt, S., Isensee, K., Telszewski, M. and Pidgeon, E.: Coastal Blue
732   Carbon: Methods for Assessing Carbon Stocks and Emissions Factors in Mangroves,
733   Tidal Salt Marshes, and Seagrasses, edited by J. Howard, S. Hoyt, K. Isensee, M.
734   Telszewski, and E. Pidgeon, International Union for Conservation of Nature, Arlington,
735   Virginia,   USA.   [online]   Available   from:
736   http://www.cifor.org/publications/pdf_files/Books/BMurdiyarso1401.pdf (Accessed 11
737   September 2019), 2014.

738   IPCC: Climate Change 2001: Third Assessment Report of the IPCC, Cambridge., 2001.

739   Islam, K. R. and Weil, R. R.: Microwave irradiation of soil for routine measurement of
740   microbial   biomass   carbon,   Biol.   Fertil.   Soils,   27(4),   408–416,
741   doi:10.1007/s003740050451, 1998.

742   Kalembasa, S. J. and Jenkinson, D. S.: A comparative study of titrimetric and
743   gavimetric methods for determination of organic carbon in soil, J. Sci. Food Agric., 24,
744   1085–1090, 1973.

745   Kauffman, B. J., Donato, D. and Adame, M. F.: Protocolo para la medición, monitoreo
746   y reporte de la estructura, biomasa y reservas de carbono de los manglares, Bogor,
747   Indonesia., 2013.

748   Kauffman, J. B., Bernardino, A. F., Ferreira, T. O., Giovannoni, L. R., de O. Gomes, L.
749   E., Romero, D. J., Jimenez, L. C. Z. and Ruiz, F.: Carbon stocks of mangroves and salt
750   marshes   of   the   Amazon   region,   Brazil,   Biol.   Lett.,   14(9),   20180208,

751 doi:10.1098/rsbl.2018.0208, 2018.

752 Kreuzwieser, J., Buchholz, J. and Rennenberg, H.: Emission of Methane and Nitrous
753 Oxide by Australian Mangrove Ecosystems, Plant Biol., 5(4), 423–431, doi:10.1055/s-
754 2003-42712, 2003.

755 Kristensen, E., Bouillon, S., Dittmar, T. and Marchand, C.: Organic carbon dynamics in
756 mangrove ecosystems: A review, Aquat. Bot., 89(2), 201–219,
757 doi:10.1016/J.AQUABOT.2007.12.005, 2008.

758 Kristjansson, J. K., Schönheit, P. and Thauer, R. K.: Different Ks values for hydrogen
759 of methanogenic bacteria and sulfate reducing bacteria: An explanation for the apparent
760 inhibition of methanogenesis by sulfate, Arch. Microbiol., 131(3), 278–282,
761 doi:10.1007/BF00405893, 1982.

762 Lekphet, S., Nitisoravut, S. and Adsavakulchai, S.: Estimating methane emissions from
763 mangrove area in Ranong Province, Thailand, Songklanakarin J. Sci. Technol., 27(1),
764 153–163 [online] Available from: https://www.researchgate.net/publication/26473398
765 (Accessed 29 January 2019), 2005.

766 Maher, D. T., Call, M., Santos, I. R. and Sanders, C. J.: Beyond burial: Lateral
767 exchange is a significant atmospheric carbon sink in mangrove forests, Biol. Lett.,
768 14(7), 1–4, doi:10.1098/rsbl.2018.0200, 2018.

769 Mahesh, P., Sreenivas, G., Rao, P. V. N. N., Dadhwal, V. K., Sai Krishna, S. V. S. S.
770 and Mallikarjun, K.: High-precision surface-level CO_2 and CH_4 using off-axis
771 integrated cavity output spectroscopy (OA-ICOS) over Shadnagar, India, Int. J. Remote
772 Sens., 36(22), 5754–5765, doi:10.1080/01431161.2015.1104744, 2015.

773 Marchand, C.: Soil carbon stocks and burial rates along a mangrove forest
774 chronosequence (French Guiana), For. Ecol. Manage., 384, 92–99,
775 doi:10.1016/j.foreco.2016.10.030, 2017.

776 McEwing, K. R., Fisher, J. P. and Zona, D.: Environmental and vegetation controls on
777 the spatial variability of CH_4 emission from wet-sedge and tussock tundra ecosystems
778 in the Arctic, Plant Soil, 388(1–2), 37–52, doi:10.1007/s11104-014-2377-1, 2015.

779 Megonigal, J. P. and Schlesinger, W. H.: Methane-limited methanotrophy in tidal
780 freshwater swamps, Global Biogeochem. Cycles, 16(4), 35-1-35–10,
781 doi:10.1029/2001GB001594, 2002.

782   Menezes, M. P. M. de, Berger, U. and Mehlig, U.: Mangrove vegetation in Amazonia :
783   a review of studies from the coast of Pará and Maranhão States , north Brazil, Acta
784   Amaz., 38(3), 403–420, doi:10.1590/S0044-59672008000300004, 2008.

785   Milucka, J., Kirf, M., Lu, L., Krupke, A., Lam, P., Littmann, S., Kuypers, M. M. M. and
786   Schubert, C. J.: Methane oxidation coupled to oxygenic photosynthesis in anoxic
787   waters, ISME J., 9(9), 1991–2002, doi:10.1038/ismej.2015.12, 2015.

788   Monz, C. A., Reuss, D. E. and Elliott, E. T.: Soil microbial biomass carbon and nitrogen
789   estimates using 2450 MHz microwave irradiation or chloroform fumigation followed by
790   direct extraction, Agric. Ecosyst. Environ., 34(1–4), 55–63, doi:10.1016/0167-
791   8809(91)90093-D, 1991.

792   Neubauer, S. C. and Megonigal, J. P.: Moving Beyond Global Warming Potentials to
793   Quantify the Climatic Role of Ecosystems, Ecosystems, 18(6), 1000–1013,
794   doi:10.1007/S10021-015-9879-4/TABLES/2, 2015.

795   Nóbrega, G. N., Ferreira, T. O., Siqueira Neto, M., Queiroz, H. M., Artur, A. G.,
796   Mendonça, E. D. S., Silva, E. D. O. and Otero, X. L.: Edaphic factors controlling
797   summer (rainy season) greenhouse gas emissions (CO2 and CH4) from semiarid
798   mangrove soils (NE-Brazil), Sci. Total Environ., 542, 685–693,
799   doi:10.1016/j.scitotenv.2015.10.108, 2016.

800   Norman, J. M., Kucharik, C. J., Gower, S. T., Baldocchi, D. D., Crill, P. M., Rayment,
801   M., Savage, K. and Striegl, R. G.: A comparison of six methods for measuring soil-
802   surface carbon dioxide fluxes, J. Geophys. Res. Atmos., 102(D24), 28771–28777,
803   doi:10.1029/97JD01440, 1997.

804   Peel, M. C., Finlayson, B. L. and McMahon, T. A.: Updated world map of the Köppen-
805   Geiger climate classification, Hydrol. Earth Syst. Sci., 11(5), 1633–1644,
806   doi:10.1002/ppp.421, 2007.

807   Poffenbarger, H. J., Needelman, B. A. and Megonigal, J. P.: Salinity Influence on
808   Methane Emissions from Tidal Marshes, Wetlands, 31(5), 831–842,
809   doi:10.1007/s13157-011-0197-0, 2011.

810   Prost, M. T., Mendes, A. C., Faure, J. F., Berredo, J. F., Sales, M. E. ., Furtado, L. G.,
811   Santana, M. G., Silva, C. A., Nascimento, I. ., Gorayeb, I., Secco, M. F. and Luz, L.:
812   Manguezais e estuários da costa paraense: exemplo de estudo multidisciplinar integrado

813   (Marapanim e São Caetano de Odivelas), in Ecossistemas Costeiros: Impactos e Gestão

814   Ambiental, edited by M. T. Prost and A. Mendes, pp. 25–52, FUNTEC and Paraense

815   Museum "Emílio Goeldi," Belém, Brazil., 2001.

816   Purvaja, R. and Ramesh, R.: Natural and Anthropogenic Methane Emission from

817   Coastal   Wetlands   of   South   India,   Environ.   Manage.,   27(4),   547–557,

818   doi:10.1007/s002670010169, 2001.

819   Purvaja, R., Ramesh, R. and Frenzel, P.: Plant-mediated methane emission from an

820   Indian   mangrove,   Glob.   Chang.   Biol.,   10(11),   1825–1834,   doi:10.1111/j.1365-

821   2486.2004.00834.x, 2004.

822   Reeburgh, W. S.: Oceanic Methane Biogeochemistry, Chem. Rev., 2, 486–513,

823   doi:10.1021/cr050362v, 2007.

824   Robertson, A. I., Alongi, D. M. and Boto, K. G.: Food chains and carbon fluxes, in

825   Coastal and Estuarine Studies, edited by A. I. Robertson and D. M. Alongi, pp. 293–

826   326, American Geophysical Union., 1992.

827   Rocha, A. S.: Caracterização física do estuário do rio Mojuim em São Caetano de

828   Odivelas   -   PA,   Federal   University   of   Pará.   [online]   Available   from:

829   http://repositorio.ufpa.br/jspui/handle/2011/11390, 2015.

830   Rollnic, M., Costa, M. S., Medeiros, P. R. L. and Monteiro, S. M.: Tide Influence on

831   Suspended Matter Transport in an Amazonian Estuary, J. Coast. Res., 85, 121–125,

832   doi:10.2112/SI85-025.1, 2018.

833   Rosentreter, J. A., Maher, D. T., Erler, D. V., Murray, R. H. and Eyre, B. D.: Methane

834   emissions partially offset "blue carbon" burial in mangroves, Sci. Adv., 4(6), 1–11,

835   doi:10.1126/sciadv.aao4985, 2018a.

836   Rosentreter, J. A., Maher, D. . T., Erler, D. V. V., Murray, R. and Eyre, B. D. D.:

837   Seasonal and temporal CO2 dynamics in three tropical mangrove creeks – A revision of

838   global   mangrove   CO2   emissions,   Geochim.   Cosmochim.   Acta,   222,   729–745,

839   doi:10.1016/j.gca.2017.11.026, 2018b.

840   Roslev, P. and King, G. M.: Regulation of methane oxidation in a freshwater wetland by

841   water   table   changes   and   anoxia,   FEMS   Microbiol.   Ecol.,   19(2),   105–115,

842   doi:10.1111/j.1574-6941.1996.tb00203.x, 1996.

843   Sahu, S. K. and Kathiresan, K.: The age and species composition of mangrove forest

844   directly influence the net primary productivity and carbon sequestration potential,

845   Biocatal. Agric. Biotechnol., 20, 101235, doi:10.1016/j.bcab.2019.101235, 2019.

846   Salum, R. B., Souza-Filho, P. W. M., Simard, M., Silva, C. A., Fernandes, M. E. B.,

847   Cougo, M. F., do Nascimento, W. and Rogers, K.: Improving mangrove above-ground

848   biomass estimates using LiDAR, Estuar. Coast. Shelf Sci., 236, 106585,

849   doi:10.1016/j.ecss.2020.106585, 2020.

850   Schmidt, M. W. I., Torn, M. S., Abiven, S., Dittmar, T., Guggenberger, G., Janssens, I.

851   A., Kleber, M., Kögel-Knabner, I., Lehmann, J., Manning, D. A. C., Nannipieri, P.,

852   Rasse, D. P., Weiner, S. and Trumbore, S. E.: Persistence of soil organic matter as an

853   ecosystem property, Nature, 478(7367), 49–56, doi:10.1038/nature10386, 2011.

854   Segarra, K. E. A., Schubotz, F., Samarkin, V., Yoshinaga, M. Y., Hinrichs, K. U. and

855   Joye, S. B.: High rates of anaerobic methane oxidation in freshwater wetlands reduce

856   potential atmospheric methane emissions, Nat. Commun., 6(1), 1–8,

857   doi:10.1038/ncomms8477, 2015.

858   Shiau, Y.-J. and Chiu, C.-Y.: Biogeochemical Processes of C and N in the Soil of

859   Mangrove Forest Ecosystems, Forests, 11(5), 492, doi:10.3390/f11050492, 2020.

860   Shiau, Y. J., Cai, Y., Lin, Y. Te, Jia, Z. and Chiu, C. Y.: Community Structure of Active

861   Aerobic Methanotrophs in Red Mangrove (Kandelia obovata) Soils Under Different

862   Frequency of Tides, Microb. Ecol., 75(3), 761–770, doi:10.1007/s00248-017-1080-1,

863   2018.

864   Sihi, D., Davidson, E. A., Chen, M., Savage, K. E., Richardson, A. D., Keenan, T. F.

865   and Hollinger, D. Y.: Merging a mechanistic enzymatic model of soil heterotrophic

866   respiration into an ecosystem model in two AmeriFlux sites of northeastern USA,

867   Agric. For. Meteorol., 252, 155–166, doi:10.1016/J.AGRFORMET.2018.01.026, 2018.

868   Souza Filho, P. W. M.: Costa de manguezais de macromaré da Amazônia: cenários

869   morfológicos, mapeamento e quantificação de áreas usando dados de sensores remotos,

870   Rev. Bras. Geofísica, 23(4), 427–435, doi:10.1590/S0102-261X2005000400006, 2005.

871   Sparling, G. P. and West, A. W.: A direct extraction method to estimate soil microbial

872   C: calibration in situ using microbial respiration and 14C labelled cells, Soil Biol.

873   Biochem., 20(3), 337–343, doi:10.1016/0038-0717(88)90014-4, 1988.

874   Sundqvist, E., Vestin, P., Crill, P., Persson, T. and Lindroth, A.: Short-term effects of

875 thinning, clear-cutting and stump harvesting on methane exchange in a boreal forest,

876 Biogeosciences, 11(21), 6095–6105, doi:10.5194/bg-11-6095-2014, 2014.

877 Valentim, M., Monteiro, S. and Rollnic, M.: The Influence of Seasonality on Haline

878 Zones in An Amazonian Estuary, J. Coast. Res., 85, 76–80, doi:10.2112/SI85-016.1,

879 2018.

880 Valentine, D. L.: Emerging Topics in Marine Methane Biogeochemistry, Ann. Rev.

881 Mar. Sci., 3(1), 147–171, doi:10.1146/annurev-marine-120709-142734, 2011.

882 Vance, E. D., Brookes, P. C. and Jenkinson, D. S.: An extraction method for measuring

883 soil microbial biomass C, Soil Biol. Biochem., 19(6), 703–707, doi:10.1016/0038-

884 0717(87)90052-6, 1987.

885 Verchot, L. V., Davidson, E. A., Cattânio, J. H. and Ackerman, I. L.: Land-use change

886 and biogeochemical controls of methane fluxes in soils of eastern Amazonia,

887 Ecosystems, 3(1), 41–56, doi:10.1007/s100210000009, 2000.

888 Wang, X., Zhong, S., Bian, X. and Yu, L.: Impact of 2015–2016 El Niño and 2017–

889 2018 La Niña on PM2.5 concentrations across China, Atmos. Environ., 208, 61–73,

890 doi:10.1016/J.ATMOSENV.2019.03.035, 2019.

891 Whalen, S. C.: Biogeochemistry of Methane Exchange between Natural Wetlands and

892 the Atmosphere, Environ. Eng. Sci., 22(1), 73–94, doi:10.1089/ees.2005.22.73, 2005.

893 Xu, X., Elias, D. A., Graham, D. E., Phelps, T. J., Carroll, S. L., Wullschleger, S. D. and

894 Thornton, P. E.: A microbial functional group-based module for simulating methane

895 production and consumption: Application to an incubated permafrost soil, J. Geophys.

896 Res. Biogeosciences, 120(7), 1315–1333, doi:10.1002/2015JG002935, 2015.

897